Molecular-Level Photoorientation Insights into Macroscopic Photoinduced Motion in Azobenzene-Containing Polymer Complexes

Mahnaz Kamaliardakani,[1] Jaana Vapaavuori,[1,†] Xiaoxiao Wang,[1] Ribal Georges Sabat,[2] C. Geraldine Bazuin,[*,1] Christian Pellerin[*,1]

[1] Département de chimie, Université de Montréal, C.P. 6128, succursale Centre-Ville, Montréal, QC, Canada H3C 3J7

[2] Department of Physics and Space Science, Royal Military College of Canada, Kingston, ON, Canada K7K 7B4

[†] Current address: Department of Chemistry and Materials Science, School of Chemical Engineering, Aalto University, Kemistintie 1, 02150 Espoo, Finland

Emails of corresponding authors: geraldine.bazuin@umontreal.ca; c.pellerin@umontreal.ca

ABSTRACT

As part of continuing efforts to deepen the understanding of photoinduced mass transport in azo-containing polymers, we compared the diffraction efficiency (DE) during surface-relief grating (SRG) inscription, photoinduced molecular orientation ($<P_2>$) and thermal stability in two sets of supramolecular azopolymer complexes; namely, hydrogen bonded (H-bonded) and ionically bonded (i-bonded) complexes, both as a function of the polymer degree of polymerization (DP). To that end, poly(4-vinylpyridine) (P4VP) of DPs 41, 480 and 1900 was H-bonded at equimolar ratio with 4-hydroxy-4′-dimethylaminoazobenzene (azoOH) and the quaternized derivatives of the three P4VPs (P4VPMe) were i-bonded via ion exchange to sodium 4-[(4-dimethylamino)-phenylazo]benzene sulfonate (azoSO_3), also known as methyl orange, where the OH functionality of azoOH is replaced by a sulfonate group. The i-bonded complexes show much better DE performance and $<P_2>$ levels than the H-bonded complexes, which we relate to the liquid crystal structure of the former complexes. Fitting of the $<P_2>$ curves by a biexponential equation leads to two parameters associated with a fast trans-cis or angular hole burning (AHB) process and a slow angular redistribution (AR) process of the azo, respectively. It is found that AHB is predominant in the H-bonded complexes, whereas the AR contribution is much greater in the i-bonded complexes, assuring their superior SRG efficiency that is enabled by the anisotropic free volume created mainly by the AR process. In each set of complexes, the SRG efficiency is much better for the lowest DP complex, while the AR contribution is constant (and low) for the H-bonded complexes and increases roughly linearly with decrease in DP for the i-bonded complexes. The latter difference might be related to the presence of entanglements in the complexes with DPs 480 and 1900, which slow down the macroscopic movement during SRG inscription but not the molecular-scale movement in photoorientation.

INTRODUCTION

Azobenzene derivatives (azos) are commonly incorporated in light-responsive materials due to their clean, efficient, and reversible photoisomerization reaction between a rod-like trans form and a bent metastable cis form.[1-4] Upon illumination with linearly polarized light, the repetitive trans-cis-trans photoisomerization cycles and angularly selective photon absorption culminate in alignment of the azo motifs perpendicular to the polarization direction of the impinging light and can lead to large and stable anisotropy in initially isotropic azo-containing materials.[1] Furthermore, light can initiate motion on a macroscopic scale in azopolymers when the sample is irradiated by an interference pattern of light. This photoinduced motion allows the formation of surface relief gratings (SRG) whose depth and diffraction efficiency depend on factors that include the nature of the azo, such as its dipole moment and cis lifetime, the laser wavelength, the type of interference pattern used, and the polymer molecular weight.[5] During SRG inscription, which is generally effected below the glass transition temperature (T_g), the azopolymer surface deforms to replicate the incident light interference pattern. The inscribed patterns can reach hundreds of nanometers in depth, indicating that polymer chains can be triggered by light to move across the substrate surface over those macroscopic distances.[1, 3, 6-8] However, despite its discovery more than two and a half decades ago[9-10] and numerous investigations since that time,[1-3, 7, 11-14] the fundamental mechanism underlying the SRG inscription process is still not comprehensively understood. Nonetheless, the SRG and photoorientation characteristics of photoactive azopolymers make them suitable candidates for various applications in photonics and optoelectronics, such as the design of rewritable holographic data recording devices,[15-16] grating waveguide couplers,[17-19] and biological tissue engineering.[20]

In the present contribution, we turn to supramolecular azopolymers to advance the understanding of SRG formation, focusing on selected molecular parameters and profiting from a molecular-level spectroscopic analysis tool. Many polymers with covalently attached azo-based side chains have been investigated in the past, but their synthesis is relatively laborious and time-consuming. Moreover, when preparing series of materials for investigations of the influence of specific molecular parameters on their optical properties, all-covalent syntheses generally do not provide identical backbone degrees of polymerization and polydispersities or an identical proportion and distribution of comotifs in the case of copolymers.[1, 15-17, 21-22] The supramolecular

approach provides a convenient alternative for facilitating fundamental chemical design studies and enabling the development of high performance photoresponsive polymer systems.[23-24] A photoactive guest molecule can be non-covalently bonded as a side group to a photopassive polymer host, notably via hydrogen (H),[25-33] ionic (i),[34-39] or halogen (X)[40-44] bonds. These supramolecular polymer azocomplexes provide fully miscible systems up to equimolar ratio of the azo to polymer repeat unit for numerous (but not all) supramolecular bonds and, as such, display the same kinds of light-induced phenomena as all-covalent systems, and in particular SRG inscription capabilities.[45] In many of these studies, the photopassive polymer host is poly(4-vinyl pyridine) (P4VP), due to its ready availability and its capacity to support all three types of non-covalent bonds, notably as an acceptor for H- and X-bonds, as well as a participant in ionic bonds when it is protonated or quaternized.

In the various studies that have been undertaken to improve the basic understanding of the photoinduced properties of azopolymers and to determine optimal designs in view of applications, two important topics have received only partial attention to date. The first is specifically related to azocomplexes, notably the effect of the interaction type and strength. The other is relevant to azopolymers in general, including azocomplexes, notably the effect of the polymer molecular weight or degree of polymerization.

In the first case, when comparing the supramolecular bond strength for a given interaction type, a direct correlation was observed between interaction strength and SRG inscription efficiency for specific H-bonded[46] and X-bonded[41] complexes. On the other hand, other investigations, involving SRG formation in films of various H-bonded and X-bonded [via iodine (I) or bromine (Br) substituents] polymer azocomplexes based on low molecular weight P4VP at relatively low azo/4VP molar ratios (0.1-0.25),[41, 47-48] gave a more complex picture. In particular, it was found that the SRG formation efficiency is significantly higher for a fluorinated I-bonded complex compared to the analogous H-bonded complex despite the higher azo-P4VP interaction strength of the latter, which was attributed to greater directionality of the halogen-P4VP bond.[41] A lower mobility, as found when comparing a lower-T_g H-bonded complex with a higher-T_g iodoethynyl-bonded complex, may also play a role.[48] In other work, a comparison of hydrogen with ionic bonding, as well as with mixed ionic/hydrogen bonding involving proton transfer, in analogous azocomplexes based on medium molecular weight poly(dimethylaminoethyl methacrylate) (PDM)

up to azo/DM molar ratios of 1.0,[49] revealed that the purely i-bonded complex (molar ratio 1.0) shows a much higher SRG inscription efficiency than the purely H-bonded complex, whereas the proton transfer complex shows somewhat better efficiency than the purely H-bonded one despite azo crystallization.

In the second case, some studies have examined the influence of the polymer molecular weight on the SRG inscription of azopolymers and azocomplexes, but results appear not to be definitive. Some reports, which involve all-covalent azopolymers,[5, 50] an azopolymer blended with a passive polymer of varying molecular weight[51] and H-bonded azocomplexes,[28] indicate that the SRG inscription efficiency and modulation depth tend to decrease with increasing molecular weight, possibly related to an increase in viscosity that hinders macroscopic chain movement.[51] The decrease occurs to a greater or lesser extent depending on the system (from very mildly[50] to rather strongly[28]), at least when beyond the oligomeric range.[28] In the case of the blend, no SRG inscription was observed when near or above the chain entanglement limit,[51] but in other azopolymers, good SRG inscription was possible in films of high molecular weight azopolymers (e.g. 400,000 g/mol).[5, 50] Moreover, rigid ionic azocomplexes based on a high molecular weight polymer backbone (quaternized P4VP of 200,000 g/mol) showed highly efficient and stable SRG formation with high modulation depths.[34-35] However, since only one molecular weight was studied, it is not clear if the SRG efficiency was high due to the type of complexation and/or other factors despite the high molecular weight, and could possibly be higher for much lower molecular weight. Or perhaps the dependence on molecular weight is different for i-bonded compared to H-bonded azocomplexes.

Here, we will compare SRG inscription in analogous H-bonded and i-bonded azocomplexes, where the molecular weight of the passive polymer is varied in both cases. In addition, we aim to contribute to a deeper understanding of the molecular mechanism underlying SRG formation by drawing correlations with molecular-level photoorientation in these complexes using time-resolved infrared (IR) spectroscopy.[48, 52,53] In particular, we take advantage of the chemical specificity of IR to determine if the orientation experienced by the azo compounds drives orientation in the photopassive polymer. These results will be related to the phenomena of angular hole burning (AHB) caused by trans-cis photoisomerization and angular redistribution (AR) involving reorientation of the trans isomers.

The azocomplexes are made using three P4VPs having low, medium and high degrees of polymerization (DPs 41, 480 and 1900, corresponding to molecular weights of 5200, 50,000 and 200,000 g/mol, respectively) and two photoactive azo molecules that differ only in the functional group designed to interact with the polymer pyridine group, as shown in **Scheme 1**. The OH-functionalized azo molecule [4-hydroxy-4′-dimethylaminoazobenzene; hereafter azoOH] interacts with the unmodified P4VP (or P) by H-bonding after simple mixing of the two components to form azoOH/P_{DP} complexes. For i-bonding, the three P4VPs are first quaternized by a methyl group (yielding P4VPMe or qP) and then subjected to an ion exchange procedure in the presence of the sulfonate-functionalized azo molecule, methyl orange {sodium 4-[(4-dimethylamino)-phenylazo]benzene sulfonate; hereafter azoSO_3}, thereby yielding the azoSO_3/qP_{DP} complexes.

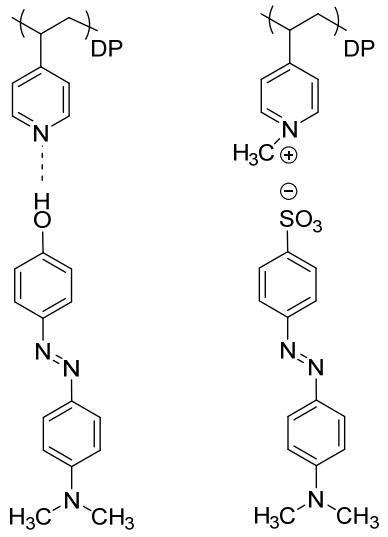

(a) azoOH/P_{DP} (b) azoSO_3/qP_{DP}

Scheme 1. Supramolecular complexes of (a) poly(4-vinylpyridine) (P4VP or P) hydrogen-bonded (H-bonded) with 4-hydroxy-4′-dimethylaminoazobenzene (azoOH) and (b) methylated poly(4-vinylpyridine) (P4VPMe or qP) ionically bonded (i-bonded) with the sulfonated analog (azoSO_3, also known as methyl orange) of azoOH. The degrees of polymerization, DP, of the polymers used are 41, 480 and 1900 in both H-bonded and i-bonded complexes.

METHODS

Materials. Poly(4-vinylpyridine) (P4VP) with a weight average molecular weight (M_w) of 5200 g/mol and a polydispersity index (M_w/M_n) of 1.20 was obtained from Polymer Source, and P4VPs with viscosity average molecular weights of 50,000 and 200,000 g/mol were obtained from Scientific Polymer Products. 4-Hydroxy-4′-dimethylaminoazobenzene (azoOH, >98%) and sodium 4-[(4-dimethylamino)phenylazo]benzene sulfonate ($azoSO_3$), commonly termed methyl orange, were obtained from Tokyo Chemical Industry and Riedel-deHaën, respectively. N,N-dimethylformamide (DMF, 99.8%), iodomethane (CH_3I, 99.5%), nitromethane (≥95%) and deuterium oxide (D_2O, 99.9%) were obtained from Sigma-Aldrich, dimethyl sulfoxide (DMSO, 99.9%) from American Chemicals, chloroform ($CHCl_3$, 99.8%) and diethyl ether (99%) from EMD Chemicals, and tetrahydrofuran (THF, 99.9%) from Fisher Scientific. All P4VPs were dried in a vacuum oven at 60 °C overnight before use, while the other chemicals were used as received. Milli-Q water was obtained from a Millipore Gradient A10 system (resistivity 18.2 MΩ.cm at 25 °C).

Complexation Procedures. The H-bonded complexes were prepared by dry mixing the appropriate amounts of azoOH and P4VP for a 1:1 azoOH:VP molar ratio, followed by dissolution in DMF at the desired concentration. These solutions were used directly for spin-coating of films. Equimolar complexation between the azoOH and the P4VP repeat units was verified by ^{1}H NMR in DMSO-d_6 (see **Figure S1a** for a representative example).

To quaternize the P4VPs for use in the i-bonded complexes, approximately 10 g of nitromethane were gradually added to 0.5 g of P4VP (5 wt%) while stirring (300 rpm) at 46 °C in an oil bath until the polymer was fully dissolved. Then CH_3I (5:1 CH_3I:VP molar ratio for P_{41} and 3:1 for P_{480} and P_{1900}) was added at once to this solution and left to stir for 5 days at 46 °C. The quaternized P4VP (P4VPMe or qP_{DP}) was precipitated by dropwise addition of the solution to about 150 mL of diethyl ether under vigorous stirring. The precipitate was filtered and left to dry overnight in a fumehood. Infrared spectroscopy (**Figure S2**) and ^{1}H NMR in D_2O (**Figure S1b**) indicated essentially full quaternization.

The i-bonded complexes were prepared similarly to the procedure described by Zhang et al.[34-35] Specifically, the desired amount of $azoSO_3$ (1.5 equivalent relative to the DP for the $azoSO_3/qP_{41}$ complex, 1.14 equivalent for the $azoSO_3/qP_{480}$ and $azoSO_3/qP_{1900}$ complexes) was

dissolved in warm DMSO (~45 °C) and maintained for at least 1 h. The qP_{41} was dissolved in DMSO (~10 mL, 120 mg/mL concentration) to which 2 mL of Milli-Q H_2O was added, whereas qP_{480} and qP_{1900} were dissolved in Milli-Q H_2O at room temperature (25 mg/mL concentrations). Then the $azoSO_3$ solution was gradually added to the qP_{DP} solution, causing precipitation. After stirring at 45 °C for 1 h, sufficient DMSO was added to re-dissolve the precipitate. To eliminate the counterions (Na^+ and I^-), DMSO and excess $azoSO_3$, the solutions were dialyzed (Spectra/Por molecular porous membrane tubing with a molecular weight cutoff 3500, from Spectrum Laboratories) against Milli-Q water for 2-3 weeks until no color was apparent in the water outside the bag, during which the Milli-Q water was refreshed several times. After dialysis, it was found necessary to further purify the $azoSO_3/qP_{41}$ complex; this was done by redissolution in DMSO and drop-by-drop precipitation in vigorously stirred Milli-Q water, followed by centrifugation in a 50-mL tube at 13000 rpm for 5 min (Sorvall RC-5C Plus Centrifuge) to maximize recovery of the complex. The final precipitates were freeze-dried for 5 d at -90 °C, followed by drying in a vacuum oven at 60 °C for 3 d and then 100 °C for 1 d. ^{1}H NMR in DMSO-d_6 indicated an essentially equimolar ratio between $azoSO_3$ and the qP repeat units (representative spectrum shown in **Figure S1c**).

Sample Preparation and Characterization. ^{1}H NMR spectra were recorded at room temperature using a Bruker Ultrashield 400 MHz spectrometer. Differential scanning calorimetry (DSC) was conducted with a PerkinElmer DSC 8500 calorimeter calibrated with indium to measure the glass transition temperatures (T_g's) of the pure P4VP samples. Samples of 2-3 mg were pressed in standard aluminum pans and vacuum-dried overnight at 70 °C. The T_g's were averaged from the half-heights of the heat capacity jump in the second and third heating scans using a heating rate of 10 °C/min from 50 to 180 °C after fast cooling. No clear T_g's could be determined for the ionic complexes despite taking scans with larger sample sizes and under different conditions (heating and cooling rates, after annealing at selected temperatures), but a T_g for the $azoSO_3/qP_{1900}$ ionic complex had been determined previously.[34-35] The T_g's for the H-bonded complexes were estimated by IR spectroscopy, as described below, in connection with another project.

Spin-coated films were prepared from DMF solutions using a Specialty Coating Systems model G3P8 spin-coater with a spin-coating time of 60 s. The solution concentrations and spin-

coating speeds depended on the desired film thicknesses or other characteristics specified below. The films were dried in a vacuum oven at 70 and 90 °C for the azoOH and azoSO_3 complexes, respectively, for 1 d to evaporate residual DMF, as confirmed by the absence of the DMF band around 1660 cm^{-1} in the IR spectra. A lower drying temperature was necessary for the H-bonded complexes to avoid losing IR-perceptible amounts of azoOH. Film thicknesses were measured with a Bruker DektakXT profilometer.

For UV-visible measurements, thin films with similar azobenzene absorbances (A) at 488 nm were spin-coated from 7 wt% DMF solutions onto BaF_2 substrates at speeds of 1100 and 1400 rpm for H-bonded and i-bonded complexes, respectively (giving A = 0.32 and 0.40, respectively). The spectra of the films were recorded with an Ocean Optics USB2000+ spectrometer equipped with a DH-mini light source. The thin films were irradiated using a linearly polarized 488-nm diode laser (JDSU FCD488-020) to induce photoisomerization in the sample for 5 min. The beam diameter of 0.7 mm was expanded to 7 mm using a Thorlabs BE10M beam expander to cover the probe beam cross section with an irradiance of ~20 mW/cm^2. The minimum cis isomer content (P_{cis}) at the end of this irradiation time was determined from **Equation 1**,

$$P_{cis} = 1 - \frac{A_{irr}}{A_0} \qquad \textbf{(Eq. 1)}$$

where A_{irr} is the maximum absorbance at the end of irradiation and A_0 the absorbance before irradiation.

Infrared Spectroscopy. For IR measurements, films with thicknesses of 500-600 nm were prepared by spin-coating 13 wt% DMF solutions onto BaF_2 windows with spin speeds varying from 300 to 1100 rpm for H-bonded complexes and 300 to 2100 rpm for i-bonded complexes, where, to obtain similar film thicknesses, the spin speed had to be increased with increasing polymer molecular weight. Five samples of each complex were prepared and analyzed to validate reproducibility. Prior to spin-coating, the azoSO_3/qP_{41} solution, which contained some precipitate, was filtered through a 0.45-μm pore-size PTFE syringe filter. The absorbances at 488 nm of all films were comparable at A = 1.5-2.

Static IR spectra were recorded using a Bruker Optics Vertex 70 Fourier transform IR spectrometer with a deuterated L-alanine triglycine sulfate (DLATGS) detector with a resolution of 4 cm^{-1} by averaging 150 scans. For comparison, spectra of the pure components were obtained

in the attenuated total reflection (ATR) mode using a Bruker Optics Tensor 27 FT-IR spectrometer equipped with a mercury cadmium telluride (MCT) detector and a MIRacle (Pike Technologies) silicon ATR accessory. The ATR spectra were recorded with a resolution of 4 cm^{-1} by averaging 256 scans on samples drop-cast directly on the ATR element from solutions of pure P_{480} in chloroform, pure qP_{480} in Milli-Q water, pure $azoSO_3$ in DMSO, and pure azoOH in THF, all at 5 wt% solution concentration.

The T_g's of the H-bonded complexes were determined by IR following our previously published approach.[54] A 1 wt% DMF solution of each complex was cast onto the single-reflection diamond element of a heated Golden Gate (Specac) ATR accessory. The samples were first heated to a maximum temperature depending on the polymer molecular weight (110, 125, and 135 °C for azoOH/P_{DP} complexes of DPs 41, 480 and 1900, respectively) for 3 min to erase thermal history. Then the IR spectra were recorded during cooling at a rate of 2 °C/min by averaging 100 scans with 4 cm^{-1} resolution using the Tensor 27 spectrometer. Background spectra were recorded for each sample by applying the same cycle. The spectroscopic T_g's were obtained by following the position of the 1362 cm^{-1} azoOH band as a function of temperature.

To probe the time-resolved photoorientation of the complexes, we used polarization modulation infrared structural absorbance spectroscopy (PM-IRSAS).[55] This method measures simultaneously the dichroic difference (ΔA) and the structural absorbance spectra (A_0), allowing the order parameter ($\langle P_2 \rangle$) to be calculated from **Equation 2**,

$$\langle P_2 \rangle = \left(\frac{2}{3cos^2\,\alpha - 1}\right)\left(\frac{\Delta A}{3A_0}\right) = \left(\frac{2}{3cos^2\,\alpha - 1}\right)\left(\frac{A_{||} - A_{\perp}}{A_{||} + 2A_{\perp}}\right) \qquad \textbf{(Eq. 2)}$$

where $A_{\parallel}$ and $A_{\perp}$ are the absorbances of the band of interest for the spectra polarized parallel and perpendicular, respectively, to the pump laser polarization, and α is the angle between the transition dipole moment of the vibrational mode and the main axis of the molecule of interest. Density functional theory (DFT) calculations were performed to estimate the angle α using Gaussian 16 on Compute Canada's supercomputer Graham. Results were analyzed using GaussView 6. All molecules were optimized with the B3LYP functional and the 6-311+G(d,p) basis set before simulating their infrared spectra. No imaginary frequencies were obtained. DFT using the same basis set was used to calculate molecular dipole moments.

PM-IRSAS spectra were recorded with a resolution of 4 cm^{-1} using the Vertex 70 spectrometer with an external optical set-up consisting of two ZnSe lenses, a KRS-5 wire-grid polarizer, a photoelastic modulator (PEM-90 type II/ZS50, Hinds Instruments), a liquid nitrogen-cooled MCT photovoltaic detector (Kolmar Technologies), a lock-in amplifier (Stanford Research Systems, SR830 DSP) with a 30-μs time constant, and two dual-channel electronic filters (Frequency Devices, 90TP/90IPB).[55] The samples were irradiated in situ for 1700 s using the beam-expanded 488-nm diode laser of ~20 mW/cm^2 irradiance also used for the UV-visible spectroscopy experiments. To follow the fast changes in orientation during the first 1 min of illumination (laser on) and of thermal relaxation (laser off), spectra were recorded from averages of 20 scans (~4 s/spectrum) and 100 scans (~19 s/spectrum), respectively. Subsequently, a higher number of scans (up to 320 scans per spectrum or ~61 s/spectrum) were coadded during the slower orientation and relaxation processes to increase the signal-to-noise ratio. Curve fitting was performed, using OriginPro 2015, on the absolute values of $\langle P_2 \rangle$.

SRG Inscription. SRGs were inscribed on spin-coated films of 400-600 nm in thickness, prepared in the same way as for the IR measurements, except using soda lime glass slides as substrates. The inscription was done using a Lexel model 95L argon-ion laser (7 W, 488 nm) at irradiances of 100, 200 and 400 mW/cm^2 (as measured with a Coherent Powerwand). The inscribing laser beam was spatially filtered, collimated, and circularly polarized by a quarter-wave plate, to have the two oppositely rotating interfering beams impinge on the sample. This combination of left- and right-circularly polarized light (LCP-RCP) produces an interference pattern with a spatially rotating linear polarization. To produce the SRG patterns, the incident laser beam was directed so that one half passed directly through the sample and the other half was reflected from a Lloyd's mirror interferometer that was installed perpendicularly to the sample to produce an interference pattern. The inscription of the SRGs was tracked during 1000 s of laser illumination by measuring the first-order diffraction of a mechanically chopped 633-nm He-Ne probe laser. The transmitted first-order diffracted signal was attenuated with a 0.4% neutral density filter before reaching the silicon photodiode to avoid detector saturation. The photodiode signal was then captured using an SRS model 830 lock-in amplifier and recorded on a computer. The diffraction efficiency (DE) was calculated by dividing the power of the first-order diffracted signal (with the pump laser on) by the power of the transmitted zeroth-order diffracted signal (with the pump laser off) obtained after completion of the SRG. To have the same input sensitivity range in

the lock-in amplifier for the zeroth-order compared to the first-order signal, a 6.6% neutral density filter was used in addition to the 0.4% filter.

RESULTS & DISCUSSION

The objective of this work is to understand the impact of binding type and polymer molecular weight on the photoinduced macroscopic mass transport of supramolecular azopolymer equimolar complexes during SRG inscription and to relate its efficiency to molecular-level photoinduced orientation. Before presenting these results, it is useful to present some basic characteristics of the complexes. Visually, the films are uniform and show no evidence of macroscopic phase separation or crystallization. The azoOH/P_{DP} films are transparent, in keeping with their amorphous non-liquid crystal (LC) structure, as shown by the absence of birefringence under polarized optical microscopy (POM).[31] In contrast, the azoSO_3/qP_{DP} films are translucent, in keeping with their (single layer) smectic A LC structure, maintained up to the onset of degradation, as determined previously by POM, X-ray diffraction, DSC and thermogravimetric analysis.[34-35] The lack of macrophase separation is indicative of a high level of complexation, since the azo molecules by themselves are crystalline with high melting points. For the H-bonded complexes, the high complexation was verified by infrared spectroscopy, which shows that the 993 cm^{-1} free pyridine band in P4VP is replaced to a large extent by the 1008 cm^{-1} H-bonded pyridine band in the complex (see section B of the Supporting Information and **Figure S3**). A previous quantitative analysis of a similar H-bonded complex over a wide range of molar ratios indicated that the H-bonding level tends to be roughly 80% of the maximum level.[53] For the i-bonded complexes, full complexation is ensured by the removal of the small counterions associated with the starting azo and polymer components.[34-35]

UV-Visible Analysis. Figure 1 shows the UV-visible spectra of thin films of the azoOH/P_{480} and azoSO_3/qP_{480} complexes before (initial state) and after 5 min of irradiation with 488-nm vertically polarized light. These spectra are representative of the complexes with all three DPs. For comparison, the spectra of the pure azos in dilute DMF solutions (0.0085 mg/mL) are also shown. The similarity between the spectra of the azoOH/P_{DP} film and the corresponding azoOH DMF solution (**Figure 1a**), in particular the wavelength of maximum absorption (λ_{max}), indicates that the azo is molecularly well dispersed in the polymer matrix with no aggregation,

consistent with the visual transparency and disordered amorphous phase of the complex. This is also an indirect indication of high complexation between the OH and VP moieties, including after irradiation, since the azoOH molecules would tend to crystallize without complexation and then drastically modify the spectrum.[48]

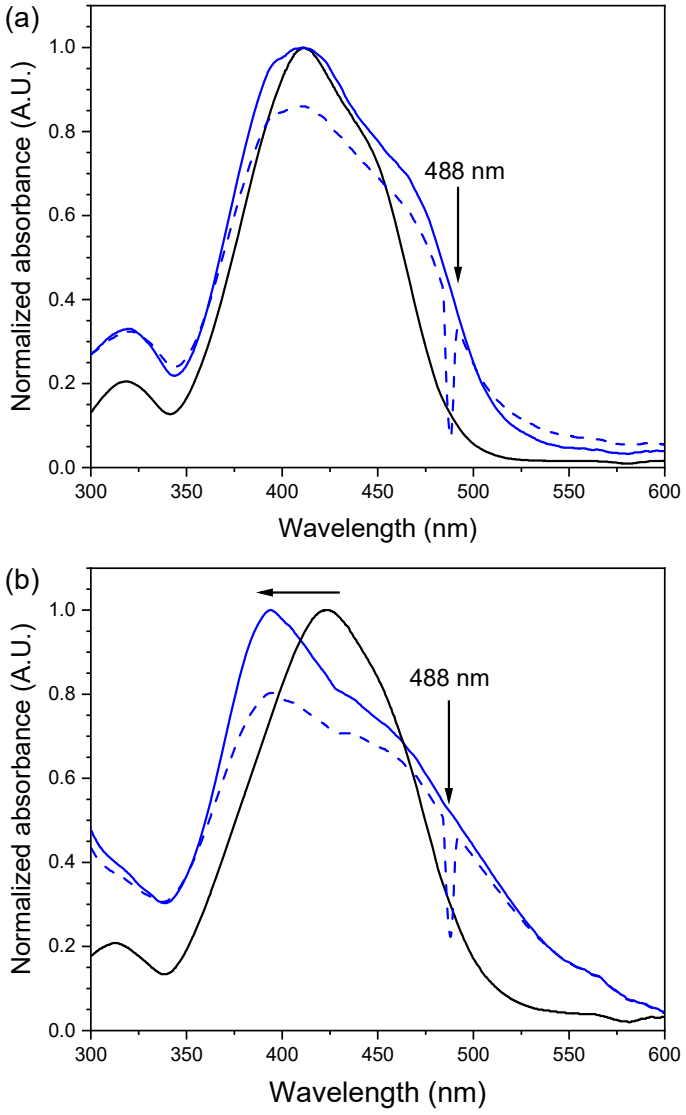

Figure 1. Normalized UV-visible absorption spectra of spin-coated thin films of (a) azoOH/P_{480} and (b) $azoSO_3/qP_{480}$ complexes before (initial state, solid blue lines) and after 5 min of irradiation (dashed blue lines), compared to the spectra of the pure azos in dilute DMF solution (0.0085 mg/mL; black lines). The dip in absorbance at 488 nm in the spectra after irradiation is caused by scattering of the laser light.

The main band at 410 nm is assigned to the π–π* absorption of the azoOH trans isomer, while the n–π* absorption of this isomer appears as a shoulder near 470 nm.[35, 49, 56] Under illumination by 488 nm light, the 410 nm band decreases in intensity as a result of trans-cis photoisomerization, and a new band due to the n–π* absorption of the cis isomer develops at around 540 nm. The extent of decrease in the 410 nm band intensity indicates, based on **Equation 1**, that the minimum cis isomer content is approximately 14% after 5 min of illumination. Since 488 nm irradiation can excite both the trans and cis n-π* azo bands, fast trans-cis-trans isomerization cycles are photochemically produced and prevent the accumulation of a large fraction of cis isomers during irradiation. Moreover, the absence of change in λ_{max} upon illumination suggests that the azo-azo interactions are not affected by the isomerization.[53]

In contrast to the H-bonded complex, the shift in λ_{max} of the UV-visible spectrum of the i-bonded azoSO_3/qP_{480} film (394 nm) compared to pure azoSO_3 in DMF (423 nm), as shown in **Figure 1b**, indicates significant differences in the chromophore-chromophore interactions between the dilute solution and the spin-coated film. This 29-nm blue shift, accompanied by differences in spectral shape, can be ascribed to changes in the local environment of the chromophore[36, 57] and to excitonic coupling of the azos due to the smectic A packing in the films.[34-35, 49] The shoulder near 450 nm in the film is most likely due to the trans n-π* transition, although it is not ruled out that it could also be due to the π–π* band of a small amount of uncomplexed azoSO_3.[35, 56, 58] The spectra of the film before and after irradiation show no change in λ_{max}, again consistent with the absence of photoinduced decomplexation, and the observed changes, notably the decrease in intensity of the 394 nm band, arise from increased cis content following irradiation. The minimum cis content after 5 min of irradiation, determined by **Equation 1** from the decrease in the absorption of the 394-nm band to be 20%, is just a little higher than that obtained for the H-bonded complex. Thus, the two systems reach a relatively low cis content under irradiation that suggests efficient trans-cis-trans isomerization cycling under similar conditions.

Glass Transition Temperature. The T_g's of the H-bonded complexes are 68, 72 and 83 °C (determined by temperature-dependent IR; see Experimental Section) in order of increasing DP. They are lower than those of the pure P4VP host, which are 134 °C for P_{41} and ~150 °C for P_{480} and P_{1900} (determined by DSC), indicating a plasticization effect of the azo as previously observed for H-bonded azopolymer complexes with P4VP.[48, 59] The T_g of the i-bonded complex

with the highest DP has previously been determined (by DSC) to be approximately 180 °C,[35] much higher than those of the H-bonded complexes. That of the intermediate DP complex is likely to be similar, while the lowest DP complex should be lower, although probably still above 150 °C, as supported by analysis of a quaternized PDM block of low molecular weight (3400) complexed with azoSO_3 (outer blocks of a microphase-separated triblock copolymer having a sub-ambient central block), for which a weak and broad T_g of 154 °C was detected.[60] In all cases, the T_g's of the complexes are well above ambient temperature.

Surface Relief Grating Formation. SRG inscription was conducted to evaluate the photoinduced macroscopic-scale mass transport in the complex films upon illumination. An interference pattern of circularly polarized 488 nm light with different irradiances (100, 200, and 400 mW/cm^2) was applied for a period of 1000 s. Examples of atomic force microscopy images of SRGs in these materials have been presented in refs 31, 34 and 35 for selected DPs (see reproductions in Figure S4). Here, we focus on the first-order diffraction efficiency (DE), which gives a more accurate picture of the inscription, being *in situ* and covering a much larger area. Using the same experimental conditions for all the samples and with small volume birefringence or polarization gratings (see below), the correlation between the surface profile amplitudes and the DE can be approximated as linear for the DE levels attained. No visual evidence of crystallization, such as increased opacity, was observed in the SRG-inscribed areas, again indicative of the robustness of the supramolecular interactions used.

Figure 2a presents the DE values as a function of time during illumination with a laser irradiance of 200 mW/cm^2 for the H-bonded and i-bonded complexes and **Figure 2b** presents these values at the end of the inscription period of 1000 s as a function of the irradiance. The DE plots show, first, that SRG inscription for each series is much more efficient for the complexes with the lowest DP (41) than for the complexes with the two higher DPs (480 and 1900), the latter being similar to each other. Second, there is a substantial difference in the SRG inscription kinetics between the H-bonded and i-bonded complexes, with the i-bonded complexes showing much more efficient SRG inscription than the H-bonded complexes, even for the highest DP i-bonded complex compared to the lowest DP H-bonded complex. This provides a more general picture that is consistent with and pulls together the more partial data in previous literature. Notably, the present data for the H-bonded complexes is consistent with previous observations that (a) the DE tends to

decrease with increasing molecular weight for all-covalent polymers and H-bonded complexes,[28, 50-51] but especially strongly in the oligomeric range (DP 41 in our case),[28] and (b) the data for the i-bonded complexes generalize those observations to include this bond type. The present data also confirm that (c) SRG inscription can nevertheless show good efficiency even for a polymer host of high molecular weight,[5, 35, 50] and that (d) i-bonded complexes perform much better than analogous H-bonded complexes.[49] It should be noted, however, that we have shown previously[35] that i-bonded complexes perform less and less well with the introduction of moieties that are increasingly flexible, such as in the azo tail, to the point that the DE curves begin to resemble those for the azoOH complexes in the present contribution.

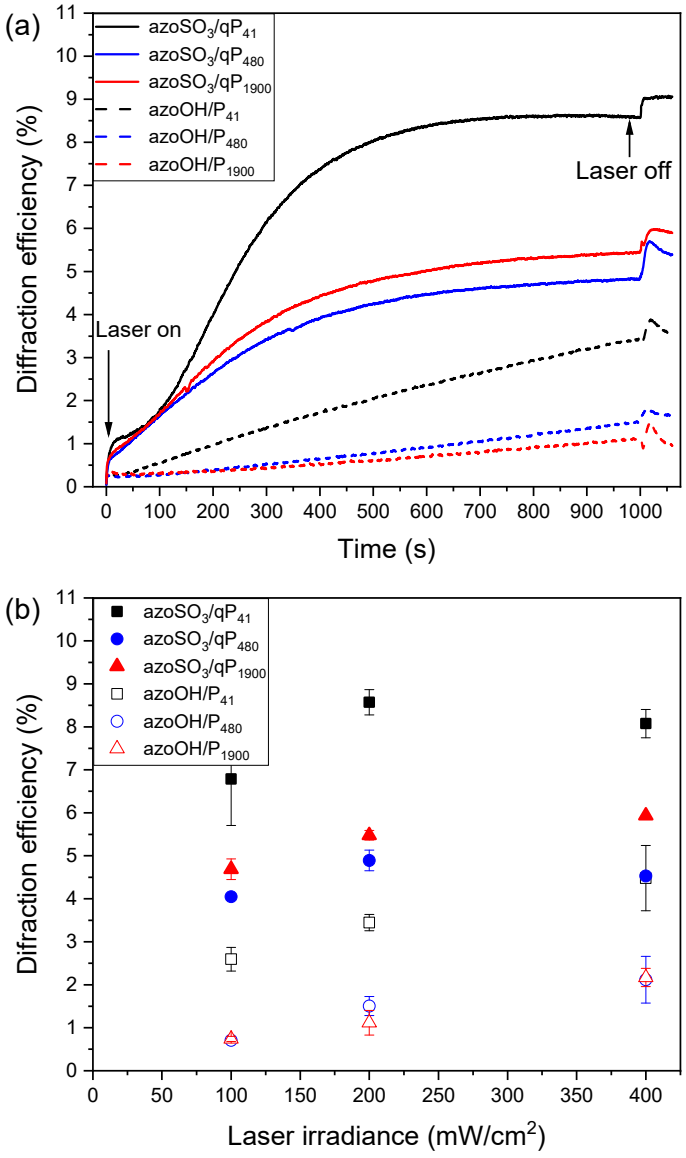

Figure 2. (a) Diffraction efficiency of surface relief grating formation as a function of irradiation time for H-bonded azoOH/P_{DP} and i-bonded azoSO_3/qP_{DP} complexes of different polymer degrees of polymerization at an irradiance of 200 mW/cm^2 (see Figure S5 for irradiances of 100 and 400 mW/cm^2). (b) Maximum DE of the azocomplexes as a function of laser irradiance (given also in Table S1), where error bars are based on measurements on 2-4 samples (one sample each for azoOH/P_{480} at 100 mW/cm^2 and for azoSO_3/qP_{480} at 100 and 400 mW/cm^2).

A closer look at the kinetics (**Figure 2a**) indicates that the DE values for the H-bonded complexes increase almost linearly during the entire 1000-s period of laser irradiation without tending towards saturation. In contrast, the DE values for the i-bonded complexes initially rise to 0.7-1% within a few seconds, then grow approximately linearly with time up to about 300 s and finally tend towards a quasi-plateau indicating (near-)saturation. Because the rates of increase in the linear portion of the curves are greater for the i-bonded complexes (from 6 to 15 times in the portion between 100 and 300 s), their 1000 s DE values are much higher than those of the H-bonded complexes despite reaching saturation relatively early on. Furthermore, the rates of linear increase in each series are similar for the two higher DP complexes and much greater (2 to 5 times) for the oligomeric (DP 41) complexes.

The effect of laser irradiance on the DE values at the end of the inscription period is shown in **Figure 2b**. For the H-bonded complexes, there is an approximately linear increase in the DE values with irradiance, on the order of 5 % increase per W/cm^2. This can be explained by the fact that the H-bonded complexes have not reached saturated DE in the 1000 s of illumination for this range of irradiances, so that higher irradiance, which results in greater SRG inscription speed (see **Figure S5b**), converts directly into larger DE values. In contrast, for the i-bonded complexes, there is an increase in DE when the irradiance is increased from 100 to 200 mW/cm^2, followed by no further change within experimental uncertainty from 200 to 400 mW/cm^2. In this case, the inscription curves have not reached saturation during the 1000 s illumination at 100 mW/cm^2 (**Figure S5a**), but they are at or close to saturation by 1000 s at 200 mW/cm^2 (**Figure 2a**) and 400 mW/cm^2 (**Figure S5b**), thereby accounting for the initial increase in DE, after which there is no further change because saturation has been reached. A similar increase in DE and a parallel change

in the temporal curve from one that continually rises to one with a plateau was observed for the i-bonded azoSO_3/PDM complexes in ref 49 when increasing the irradiance from 50 to 190 mW/cm^2.

Finally, we draw attention to the changes in DE at the start and at cessation of irradiation (**Figure 2a**). The initial rapid increase in the first few seconds, which reaches approximately 0.2% and 1% at 200 mW/cm^2 for the H-bonded and i-bonded complexes, respectively, is attributed to volume birefringence gratings.[61] Subsequently, their growth is overtaken by mass transport of the material resulting in the SRGs. This is accompanied by a decrease in the rate of DE increase compared to the first seconds of irradiation and in some cases to a decrease in the absolute DE value for azoOH/P_{DP}, which suggests that the transient and permanent gratings do not diffract in phase.[61] Upon cessation of irradiation at 1000 s, a small increase in the DE values is observed, which is attributed to the back relaxation from cis to trans or the elimination of the volume birefringence grating in favor of the strongly diffracting surface relief gratings.[62] The diffraction from the volume birefringence grating is out-of-phase with the diffraction from the SRG, thereby diminishing the total diffracted signal during the irradiation period. Its rapid disappearance upon cessation of irradiation increases the DE arising from the more permanent SRG.[61]

Photoinduced Orientation. To gain molecular-level insight into the SRG inscription process, we used PM-IRSAS to investigate photoinduced orientation (expressed as the order parameter $\langle P_2 \rangle$) over time of the azo chromophores and the polymer hosts under linearly polarized illumination, followed by thermal relaxation. For the azoOH/P_{DP} complexes, two azoOH bands that are sufficiently isolated and intense to provide a good signal-to-noise ratio lie at 1363 and 1148 cm^{-1} (see **Figure S6a**, which compares the ATR spectra of the pure components with the structural absorbance (A_0) and dichroic difference (ΔA) spectra under irradiation of a spin-coated film of azoOH/P_{480}). According to DFT calculations, the band at 1363 cm^{-1} is due to a complex mode involving the dimethylaminophenyl moiety, while the 1148 cm^{-1} band involves in-plane deformation of the aromatic C–H and C−N bonds. For P4VP, the most isolated bands are those at 1418 and 1008 cm^{-1}, which can be assigned to an antisymmetric C–H deformation of the pyridine ring and to a symmetric ring deformation of the H-bonded P4VP, respectively. For the i-bonded complexes, the intense 1365 and 1113 cm^{-1} azoSO_3 bands and the 1643 cm^{-1} P4VPMe band are suitable choices (see **Figure S6b**). According to DFT calculations, the 1365 cm^{-1} band is the azoSO_3 equivalent of the azoOH 1363 cm^{-1} band, the 1113 cm^{-1} band is due to a highly delocalized

vibration of the azo molecule, while the 1643 cm^{-1} P4VPMe band can be assigned to a symmetric stretching mode of the pyridinium ring. The α angles for the selected bands, needed to calculate the $<P_2>$ values with **Equation 2**, were estimated with the help of DFT calculations. The vibrational modes of azoOH and azoSO_3 all involve transition dipole moments parallel to the azo long axis, implying that $\alpha \sim 0°$. Those of the 1008 cm^{-1} P4VP band and of the 1643 cm^{-1} P4VPMe band are parallel to the N-C4 axis of the pyridine ring so that $\alpha \sim 0°$, whereas $\alpha \sim 90°$ for the 1418 cm^{-1} P4VP band (the transition dipole moment is perpendicular to the N-C4 axis but in the plane of the pyridine ring).

Figure 3 gives the $<P_2>$ values determined from the 1363 cm^{-1} azoOH band and the 1365 cm^{-1} azoSO_3 band as a function of time during irradiation at 488 nm (laser on) followed by thermal relaxation (laser off) for the two series of complexes. These curves are compared with the 1148 cm^{-1} azoOH band and the 1113 cm^{-1} azoSO_3 band in **Figure S7a**,**b**, showing that the two bands for each azo give very similar results in terms of both the shape of the curves and the amplitude of the order parameters.

We will focus first on the photoorientation part of the curves. The initial $<P_2>$ values before illumination are close to zero because of the random distribution of the trans azobenzenes in the spin-coated films. Upon irradiation, $<P_2>$ first grows rapidly towards negative values, which is consistent with the expected perpendicular orientation of the azo molecules relative to the polarization direction of light. For the H-bonded complexes, the photoorientation reaches a quasi-plateau after a few seconds of irradiation, corresponding to the saturation level of orientation ($<P_2>_{max}$). In contrast, for the i-bonded complexes, the photoorientation of azoSO_3 increases in a biexponential fashion, where the initial fast process is followed by a slow process that does not reach a saturated $<P_2>_{max}$ within the timescale of the experiment. The $<P_2>$ values are similar for both series of complexes during the fast process; however, at the end of irradiation, the i-bonded complexes reach much higher $<P_2>$ values, on the order of -0.14 compared to around -0.045 for the H-bonded complexes, because of the contribution of the slow process. Interestingly, the $<P_2>_{max}$ values reached by a given azo, tabulated in **Table 1**, vary little with the polymer DP, contrasting with the DP dependence of the SRG results, which will be discussed later.

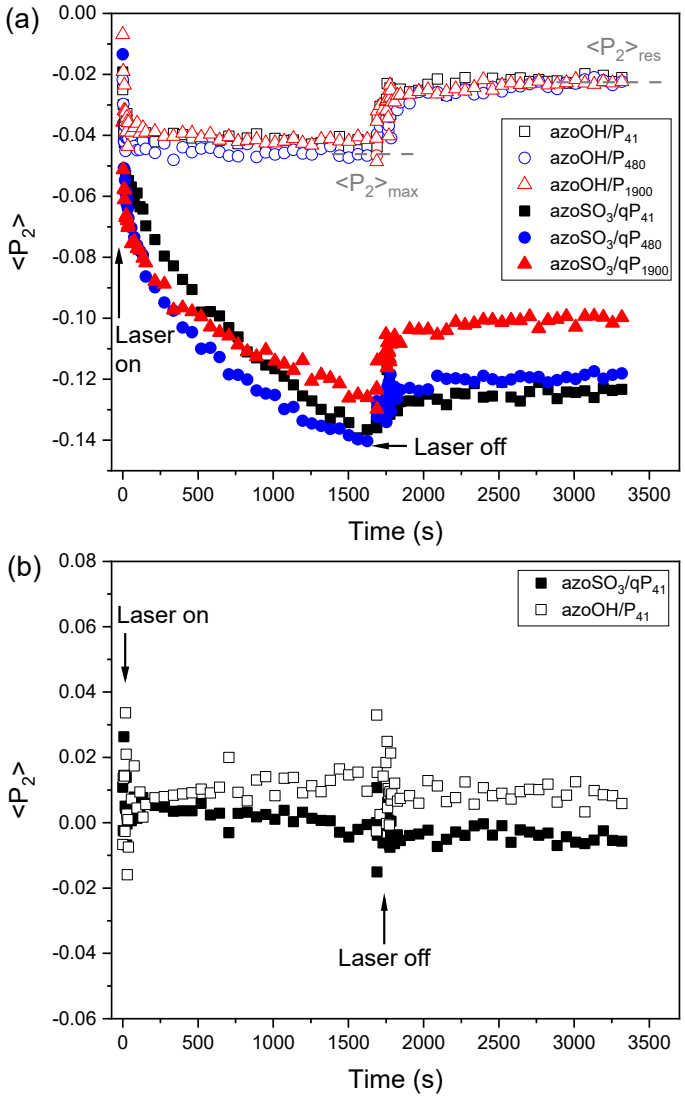

Figure 3. Photoinduced orientation (laser on) and thermal relaxation (laser off) curves of (a) the azo unit in the azoOH/P_{DP} and azoSO_3/qP_{DP} complexes and (b) the host polymer in the azoOH/P_{41} and azoSO_3/qP_{41} complexes.

Table 1. Maximum azobenzene orientation ($<P_2>_{max}$) and percentage of residual orientation ($<P_2>_{res}$) after thermal relaxation, determined using the indicated bands for the H-bonded and i-bonded complexes.

	$<P_2>_{max}$		$<P_2>_{res}$ (%)[a]	
azoOH/P_{DP}	1148 cm^{-1}	1363 cm^{-1}	1148 cm^{-1}	1363 cm^{-1}
41	-0.043 ± 0.004	-0.043 ± 0.004	47 ± 2	50 ± 3
480	-0.046 ± 0.004	-0.047 ± 0.005	47 ± 7	48 ± 9
1900	-0.043 ± 0.003	-0.041 ± 0.002	50 ± 5	54 ± 5
azoSO_3/qP_{DP}	1113 cm^{-1}	1365 cm^{-1}	1113 cm^{-1}	1365 cm^{-1}
41	-0.14 ± 0.01	-0.14 ± 0.01	92 ± 2	90 ± 3
480	-0.14 ± 0.01	-0.14 ± 0.01	87 ± 3	85 ± 2
1900	-0.13 ± 0.01	-0.13 ± 0.01	80 ± 2	80 ± 2

[a] Residual orientation, $<P_2>_{res}$, is expressed as the percentage of the $<P_2>$ value after 1700 s of thermal relaxation relative to the maximum orientation, $<P_2>_{max}$.

The fast photoorientation process is related to a phenomenon called angular hole burning (AHB), during which there is a rapid depletion of trans azos that are parallel or partly parallel to the laser polarization direction.[63-66] Indeed, the probability of photon absorption is proportional to the cosine squared of the angle between the electronic transition dipole moment of the azo and the laser electric field vector. This leads to a fast apparent perpendicular orientation due to the angularly selective photoisomerization to the cis state. Therefore, the steep drop in the $<P_2>$ values for azoOH during the first few seconds of irradiation immediately followed by a quasi-plateau strongly suggests that the photoorientation in the azoOH/P_{DP} complexes is dominated by the AHB process. On the other hand, the slow orientation process that follows the rapid AHB for the azoSO_3/qP_{DP} ionic complexes is ascribed to a mechanism of angular redistribution (AR) involving multiple trans-cis-trans isomerization cycles. This process progressively reorients the long axis of the trans isomer and culminates in their accumulation perpendicular to the laser polarization direction.[53, 66-68] It may be added that, when sufficiently strong intermolecular interactions are

present, AR can involve cooperative reorientation of an indeterminate number of neighboring molecules.

The relative importance of the AHB and AR processes can be estimated by fitting the photoorientation curves with a biexponential function[69-70] (**Equation 3**),

$$\langle P_2 \rangle = A\left[1 - e^{\left(-\frac{t}{\tau_A}\right)}\right] + B\left[1 - e^{\left(-\frac{t}{\tau_B}\right)}\right] \qquad \textbf{(Eq. 3)}$$

where the parameters A and B represent the contributions of the fast (AHB) and slow (AR) modes to the photoorientation process with time constants τ_A and τ_B, respectively. Examples of curve fits for each type of complex are illustrated in **Figure S8a**,**b**. The resulting τ_A and τ_B values and the relative contributions of AHB and AR processes to the photoorientation are shown in **Table 2**.

Table 2. Parameters obtained by fitting the photoorientation curves in Figure 2 using **Equation 3**.[a]

	DP	τ_A (s)	τ_B (s)	A_n (%) [b]	B_n (%) [b]
azoOH/P$_{DP}$	41	2 ± 1	170 ± 8	87 ± 6	13 ± 6
	480	3 ± 1	150 ± 2	88 ± 8	12 ± 8
	1900	8 ± 1	470 ± 20	88 ± 4	12 ± 4
azoSO$_3$/qP$_{DP}$	41	8 ± 1	1110 ± 70	31 ± 2	69 ± 2
	480	7 ± 1	660 ± 30	42 ± 3	58 ± 3
	1900	3 ± 1	620 ± 30	51 ± 1	49 ± 1

[a] The values and uncertainties represent the means and standard deviations of the parameters obtained when curve fitting the photoorientation curves of six different films for each complex.

[b] $A_n = \left(\frac{A}{A+B}\right) \times 100$ and $B_n = \left(\frac{B}{A+B}\right) \times 100$

Table 2 indicates that the AHB process (A_n) in the photoorientation of the H-bonded complexes is predominant at about 85-90%, thus with a contribution from the slow AR component (B_n) that is only about 10-15%. The AHB process occurs on a timescale (τ_A) on the order of a few

seconds (from 2 to 8 s). The characteristic time for the slow AR component (τ_B) is necessarily much longer, although the values in **Table 2** are not accurate given its small contribution to the photoorientation process. Moreover, the AHB and AR contributions for the H-bonded complexes are independent of the molecular weight of the host polymer. In the i-bonded complexes, the AR contribution to the photoorientation is much larger at 50-70%. The characteristic times for the fast AHB process are in the same range as for the H-bonded complexes, whereas these times for the slow process are on the order of 10 min or more. Significantly, the AR contribution to the photoorientation of the i-bonded complexes decreases (and concomitantly the AHB contribution increases) with increase in polymer DP. In this context, the apparent lack of a $<P_2>_{max}$ dependence on DP for the ionic complexes mentioned above can be viewed as more or less coincidental considering the following. The increasing AHB contribution to $<P_2>$ as DP increases, which dominates only at short irradiation times, is gradually offset by the AR contribution with DP as the irradiance time lengthens. This causes the $<P_2>$ value for the lower DP to gradually approach that for the higher DP, and, for long enough irradiance time, to surpass the $<P_2>$ value for the higher DP. This is particularly apparent in the curves for DP 41 (**Figures 3a** and **S6**), where at 1700 s of irradiance the $<P_2>$ values for DP 41 have already surpassed the values for DP 1900 and are about to surpass the values for DP 480. These tendencies would probably be more apparent at the higher irradiances used for SRG inscription.

Upon cessation of irradiation, relaxation of orientation occurs for both sets of complexes, as shown in **Figure 3a**. Like photoorientation, it is characterized by an initial fast process in the first few seconds that can be understood as a reversal of the AHB process, in that cis isomers thermally relax back to the trans form, at least partially.[69-70] Then, an extremely slow process sets in so that the order parameter quickly reaches a quasi-plateau that is indicative of the residual orientation, $<P_2>_{res}$, that remains in the films. Because the slow process hardly affects its level, the value of $<P_2>_{res}$ relative to $<P_2>_{max}$ in the relaxation timescale studied is determined essentially by the extent of AHB reversal; i.e. the lower the $<P_2>_{res}$ relative value, the greater the extent of AHB relaxation that occurs. That the slow process observed in photoorientation (driven by the laser) hardly contributes to the thermal relaxation can be rationalized by the fact that the systems are well below their T_g. **Table 1** shows that the percentages of $<P_2>_{res}$ measured at 1700 s of relaxation are much higher for the i-bonded complexes (80-90%) than for the H-bonded complexes (around

50%), indicating that the i-bonded complexes are more efficient than the H-bonded complexes in preserving their photoorientation.

Furthermore, no dependence of the percent $<P_2>_{res}$ on the polymer DP is apparent for the H-bonded complexes, in parallel to the observations for $<P_2>_{max}$ and its AHB and AR contributions (**Figure 3a** and **Table 1**). In contrast, the percent $<P_2>_{res}$ for the i-bonded complexes decreases with increase in DP, which is consistent with the increasing degree of the AHB contribution and decreasing degree of the AR contribution to photoorientation with DP in the i-bonded complexes (**Table 2**). Thus, the ionic azoSO_3/qP_{41} complex shows the greatest AR efficiency, which, in turn, leads to a higher proportion of photoorientation that resists relaxation, culminating in higher residual orientation.

The percent $<P_2>_{res}$ trends discussed above are all consistent with the relative importance of the fast AHB process to photoorientation. However, comparison of **Tables 1** and **2** indicates that the percent $<P_2>_{res}$ values are systematically larger than the related AHB fractions. This suggests that a significant proportion of the AHB orientation is not recoverable on the timescale of several min of thermal relaxation well below T_g. Under laser irradiation, the cis-trans reaction can occur thermally and photochemically because the cis conformer also absorbs at the illumination wavelength. When the irradiation is stopped, only the slower thermally activated cis-trans reaction can take place. It is thus plausible that a number of cis conformers remain kinetically trapped by the rigid matrix or relax to an oriented trans conformation because of steric constraints, thereby contributing to the high percent $<P_2>_{res}$ values in addition to the stable AR orientation.

In contrast to the azo bands, **Figure 3b** shows the $<P_2>$ values of the pyridine bands for the H-bonded complex and of the pyridinium band for the i-bonded complex show no clear variation over time during illumination (and therefore none either after cessation of illumination). Static polarized spectra recorded after 1000 s of irradiation, shown in **Figure S9a**,**b** for the H-bonded and i-bonded complexes of DP 480, confirm that no significant orientation is observable for the pyridine or pyridinium side group. This implies that the orientation of the azo derivatives does not drive a measurable orientation of the passive polymers in the present complexes, which is similar to what was found in some systems[53] but contrasts with some other systems,[48, 53] as discussed below.

Discussion. It is instructive to compare the PM-IRSAS photoorientation results of the present contribution, particularly those contrasting the H-bonded and i-bonded complexes, with those obtained by us under similar irradiation conditions for a previous system,[53] where two H-bonded complexes analogous to the present azoOH but with different tail substituents, namely H and CN in the place of dimethylamino (DMA), were investigated. In this comparison, we will use the acronyms, DMAazoOH, HazoOH and CNazoOH, respectively, to distinguish the H-bonded complex of the present contribution and those of ref 53. We will also refer mainly to the present complexes that have a P4VP DP of 1900 since this was the only DP studied in ref 53 and to the equimolar complexes in ref 53 since this was the only azo/VP composition studied in the present paper.

There are several striking parallels between the DMAazoOH and HazoOH complexes on the one hand, and the azoSO$_3$ and CNazoOH complexes on the other hand. First, the shape of the photoorientation curves for the DMAazoOH and HazoOH complexes are very similar, notably with the rapid development of a plateau, and the shape of these curves for azoSO$_3$ and CNazoOH complexes are similar, showing a continuous rise within the irradiation period (1600-1800 s). Furthermore, the maximum orientation at the end of the irradiation period for azoSO$_3$ and CNazoOH complexes are much greater (3 and ~4 times, respectively) than that for DMAazoOH and HazoOH complexes. In parallel, the AR contribution is important (50-70%) for the azoSO$_3$ and CNazoOH complexes, whereas the AHB contribution is predominant (~90%) for the DMAazoOH and HazoOH complexes. Moreover, there is relatively little thermal relaxation for the azoSO$_3$ and CNazoOH complexes ($<P_2>_{res}$ ~80%), whereas orientation is less stable for the DMAazoOH and HazoOH complexes ($<P_2>_{res}$ ~50% or less).

The parallels between the DMAazoOH and HazoOH complexes and between the azoSO$_3$ and CNazoOH complexes cannot be ascribed to the nature of the supramolecular bond, since three involve the H-bond and only one involves the i-bond. Nor can it be ascribed to T_g differences, since the T_g's are similar for all three H-bonded complexes (below 100 °C; see above) and much higher for the i-bonded complex (near 180 °C; see above). On the other hand, both the DMAazoOH and HazoOH complexes are isotropic, whereas the azoSO$_3$ and CNazoOH complexes have a LC structure.[31,34-35] This strongly suggests that the main reason for the differences between the two pairs of complexes lies in their phase state, or more fundamentally in the strength of the lateral interactions between the azo groups that give rise to the LC order. These lateral interactions are

determined by factors such as the azo dipole moment and steric features that may favor or inhibit LC packing. The correlation with LC order is further supported by the observation in ref 53 that the maximum orientation for the CNazoOH complex is 3-5 times greater than for the HazoOH complex only when the degrees of complexation with P4VP are greater than about 35%, which is also the minimum degree of complexation required to have LC order, whereas the two complexes have similar maximum orientation and orientation stability for lower degrees of complexation where both are amorphous and lack significant azo-azo interactions.[31,53] It is also noteworthy that there appears to be a correlation between the relative $\langle P_2 \rangle_{res}$ after thermal relaxation and the dipole moment, μ, calculated by DFT for the azos of the H-bonded complexes. Notably, the relative $\langle P_2 \rangle_{res}$ increases from ~10% for HazoOH (μ = 1.6 D) to ~50% for DMAazoOH (3.8 D) to ~75% for CNazoOH (6.8 D). Furthermore, while the dipole moment of azoSO_3 cannot be calculated with confidence due to its ionic nature, the fact that this system provides the largest $\langle P_2 \rangle_{res}$ (80%) is consistent with an expected high dipole moment. The importance of LC order, and azo-azo interactions in particular, can be understood in terms of a cooperative effect in the AR process,[1] notably that AR can involve the concerted reorientation of many azo groups together as a consequence of those interactions. The length scale of cooperative reorientation likely depends, among other factors, on the azo-azo interaction strength or azo dipole moment as well as sample preparation method and thermal history, and may be associated with LC domains, noting however that these domains may be poorly defined in the i-bonded complexes with their SmA structure and especially intrinsically very high T_g.

Interestingly, the parallels between the present results and ref 53 extend incompletely to the orientation of P4VP. In both cases, no P4VP orientation was observed for the isotropic H-bonded complexes of DMAazoOH and HazoOH, related in ref 53 to the predominance of AHB in the azo photoorientation whereas significant AR was required to induce orientation in the passive P4VP side group. However, here we likewise observed no P4VP orientation for the ionic complexes, in contrast to the CNazoOH complex for which it was present. The absence of P4VP orientation in the ionic complexes despite an AR contribution that is similar to that for the CNazoOH complex may be related to the non-directionality of ionic bonds (though subject to steric factors not significantly increasing the ionic bonding distance). Consequently, as the azo groups reorient under irradiation, the pyridinium groups that follow the sulfonate groups when they move have significant positional latitude that may favor their maintaining isotropic conformation. In

contrast, the H-bond is directional, with the consequence that the VP segments try to orient with respect to the azo AR to maximize the H-bond strength, thereby resulting in some degree of VP orientation. This interpretation is supported by our previous observation of higher VP orientation when the azobenzene is complexed via a halogen (I) bond in the place of a hydrogen bond,[48] consistent with the still higher directional nature of the X-bond. It should be mentioned that, in refs 48 and 53, the orientation of the polymer was limited to the pyridine side groups and did not extend to the main (hydrocarbon) chain. It is also noteworthy that modest main chain orientation was observed for poly(Disperse Red 1 acrylate) despite its capability of creating SRGs with high diffraction efficiency[51, 71] and that macroscopic mass transport was recently observed[7] without any orientation under irradiation of a single beam of sufficiently high irradiance.

The question now arises as to how the PM-IRSAS results concerning molecular-scale photoorientation can shed light on the macroscopic-scale SRG phenomenon, considering that molecular motion must underly macroscopic motion. It should be kept in mind, however, that the 5- to 20-fold difference in irradiance used for the two sets of experiments must be taken into account. For example, with reference to **Figure 2b**, if the SRG inscriptions had been done at 20 instead of 200 mW/cm^2, they would not have shown a tendency towards a plateau even for the i-bonded complexes, as found in ref 49. Nevertheless, it is possible to make certain correlations and to comment on several aspects.

At the earliest stage of irradiation, the AHB process induces rapid trans-cis isomerization and an apparent orientation due to the angular selection (e.g. **Figure 3a**).[63-65, 69] AR orientation may also develop rapidly at the high (100-400 mW/cm^2) irradiance used for SRG inscription. Indeed, photoorientation studies on low molecular weight azomaterials at 100 mW/cm^2 irradiance show that a plateau in $\langle P_2 \rangle$ is reached quickly and that it is difficult to separate the AHB and AR processes.[72] These combined effects can explain the rapid rise in DE in the first few seconds of SRG inscription (e.g. **Figure 2a**) leading to the formation of bulk birefringence gratings. The much larger initial rise observed for the azoSO$_3$/qP complexes compared to the azoOH/P complexes, is consistent with their higher $\langle P_2 \rangle_{max}$ values. The higher cis fraction (20% vs. 14%), as well as a possibly larger difference in refractive index between the grating regions, may also contribute to the higher DE rise for the azoSO$_3$/qP complexes. Moreover, the results of **Figure S5** indicate a somewhat lower (higher) initial DE rise at lower (higher) irradiance, as expected. The absence of clear dependence of this initial DE rise on DP is qualitatively consistent with the similar

photoorientation results within each complex series. It is more speculative to draw quantitative correlations between the intensities of the AHB and AR processes and the fast DE rises, given the experimental uncertainties (both in the data acquisition and in the curve fitting), phase relations between the diffraction from these bulk birefringence gratings and the already forming SRGs, and the irradiance differences. Immediately after the irradiation is stopped, the thermal cis-to-trans relaxation partly reverses the effects of AHB that took place during photoorientation, resulting in a rapid rise in DE, consistent with the temporary nature of the bulk grating.

The SRG inscription *per se* requires anisotropic macroscopic motion of the complexed azo and polymer, so that the PM-IRSAS observations must be transposed indirectly to the SRG conditions. It seems clear that the anisotropic macroscopic motion is made possible by the AR process since the azo reorientation relative to the impinging light polarization intrinsically involves molecular movement. This anisotropic motion can be associated with the impact of irradiation on the free volume in the system. Several studies have shown experimentally that photoinduced free volume plays a key role in light-induced motion in azomaterials and that the "photosoftened" material can be manipulated, for instance, through optical tweezers.[12, 51, 73-74] A detailed model recently published by Sekkat provides a quantitative connection between the absorbed energy dose and the photoinduced decrease in relaxation time, analogous to the effect of temperature on non-irradiated systems.[8] Our group, in an infrared spectroscopy investigation, showed that the photoisomerization of the azobenzene under unpolarized light strongly perturbs the chemical environment around the azo, as expected, whereas it does not affect the chemical environment of molecular moieties located far from the azo such as the polymer chain in the case of a covalent sidechain azopolymer.[54] This observation was associated with a submolecular-scale gradient of photoinduced free volume, which is the greatest around the azo and the least around the polymer main chain. When polarized light is used, the photogenerated free volume becomes anisotropic due to the azo orientation.[8] This free volume is filled in again by the azo when it undergoes cis-trans conversion and/or by neighboring molecules, including polymer segments. If the azo orientation is only of the AHB type, the anisotropic free volume is more likely to be filled by the azo that created it in the first place because the illumination drives both (fast) trans-cis and cis-trans photochemical conversions. In this case, the more slowly moving neighboring azo molecules or polymer segments cannot occupy that free volume as effectively, thereby leading to lower SRG inscription efficiency. In contrast, the AR process occurs on a longer time scale, so that

neighboring azo molecules and polymer segments have the time to occupy the created free volume more efficiently. We believe it is this process of azo orientation followed by material movement to fill in the photoinduced anisotropic free volume in a directional manner, when repeated over multiple cycles, that enables anisotropic macroscopic motion. It can occur even if $\langle P_2 \rangle$ in the photoorientation curves has reached a (quasi-)plateau, as may well be the case for the ionic complexes at the irradiances used for SRG. The AR process is likely enhanced by the above-mentioned cooperative effect that is greater the stronger the intermolecular interactions. Furthermore, although the macroscopic motion may involve polymer orientation, as found in ref 53, the present work on the i-bonded complexes indicates that this is not a necessary corollary.

The above discussion rationalizes the clear correlation between the much more efficient DE and the much larger AR contribution to photoorientation in the i-bonded complexes compared to the H-bonded complexes. On the other hand, this correlation does not hold as a function of DP. Here, the DEs are most efficient for the lowest DP and similar for the two higher DPs, whereas the AR contribution appears independent of DP for the H-bonded complexes and decreases roughly linearly with DP for the i-bonded complexes. This can be related to the different mobility length scales of AR and SRG inscription. Notably, AR is a more localized phenomenon, even though it can occur at a significantly larger scale than AHB due to the cooperative effect, whereas SRG is a macroscopic phenomenon involving long-range flow, i.e. the capacity of polymer chains to diffuse. This implies that the latter is much more dependent on the degree of polymer entanglement than the former. Thus, DP 41, being oligomeric, is too short to form an entangled network, whereas it is expected to be present for DPs 480 and 1900, which explains why DP 41 stands out in its SRG efficiency. Furthermore, the irradiance ranges used to drive photoorientation (AR and AHB) and SRG formation typically differ by an order of magnitude (including this study), indicating that driving the global mass transport of polymer chains requires significantly more accumulated energy than driving chromophore motion at the length scales required for efficient AR. In this connection, given that the AR contribution to photoorientation in the H-bonded complexes is low, the differences in this contribution as a function of DP may be too small to observe experimentally at the low irradiance used, but may become more obvious at the higher irradiances used for SRG inscription. There also appears to be an anomaly between the significant AR contribution for the CNazoOH complex in ref 53 (and discussed above) and the lack of significant SRG observed for this same complex in ref 31, which should be revisited.

From a more general perspective, the SRG writing efficiency and photoorientation depend on 1) the capacity of the azobenzenes to undergo AR and 2) the capacity of the complexed polymer (neighboring molecules and segments) to occupy the anisotropic free volume. As discussed earlier, the former increases with stronger azo-azo interactions, especially when a LC phase is formed such as for the CNazoOH and azoSO_3 complexes. Increasing the irradiance enables more photoisomerization events per unit time and therefore faster SRG inscription kinetics and higher DE, at least until a plateau is reached. The second aspect is dependent on the intrinsic flexibility of the polymer, the T_g, the effective degree of entanglement (for SRG), etc. Moreover, photoorientation and SRG inscription is countered to some extent by simultaneously occurring relaxation processes, which are also affected by factors such as molecular flexibility, T_g and DP. For example, a lower T_g or greater molecular flexibility increases the capability of the azo to orient by making the matrix less resistant, but it also speeds up orientation relaxation, typically leading to lower plateau values for orientation.[35, 48, 72]

Our previous work on azo-containing molecular glasses, which are devoid of entanglements and therefore present a more direct correlation between their molecular-scale and macroscopic-scale motions than azopolymers do, has shown that the saturated DE (reached in all cases) decreases when the matrix is too mobile, attributed to the competing effects of SRG inscription and relaxation.[52] This led to a correlation between the saturated DE value and the resistance to orientation relaxation, as expressed by $<P_2>_{res}$ values, in systems where the T_g of the matrix can be changed while maintaining fixed most other molecular and photochemical aspects.[52, 72] A relation between orientation stability and DE can also be found in the results of Zhang et al., where quaternized P4VP was complexed by ionic bonding to a series of azoSO_3 analogues.[35] AzoSO_3 derivatives with a small or rigid tail group (DMA, H or methyl) provided a remnant birefringence, a quantity related to $<P_2>_{res}$, of 95% or more. Consequently, these three complexes produced SRGs with a high DE that tended toward the same plateau. In contrast, the compound with a flexible *n*-hexyl tail had a lower remnant birefringence (~80%) and the DE of its grating was ~4 times lower, whereas the compound with a bulkier 2-methylbutyl tail showed intermediate behavior. A similar trend was found here for azoSO_3/qP_{DP}, but it is not possible to conclude in the case of azoOH/P_{DP} because its slow inscription kinetics did not allow reaching saturated DE values.

In future research, it is of interest to pursue parallel investigations of SRG inscription and photoorientation by PM-IRSAS, and thereby determine additional relationships between DE and the AHB vs. AR processes. In particular, further insight is probable in studies comparing analogous complexes where both the H-bonded and i-bonded systems are disordered, and, on the contrary where both are LC, and this for low and high DP. It is also desirable to investigate both types of experiments at various irradiances including where at least some are identical for both experiments. Lower azo/(polymer repeat unit) ratios, particularly for a system such as the CNazoOH complex where LC character sets in above a certain ratio, and analogous all-covalent systems could be included in the comparisons.

CONCLUSIONS

Through a parallel investigation of macroscopic-scale SRG inscription and molecular-scale photoorientation by PM-IRSAS in supramolecular polymer complexes, we have determined some relationships governing the effects of the type of supramolecular bond and of the degree of polymerization. SRG inscription was found to be much more efficient for the ionically bonded (i-bonded) complexes than for the H-bonded complexes studied. In both cases, the oligomeric complexes show significantly greater efficiency than the higher molecular weight polymeric complexes, although the highest molecular weight i-bonded complex still performs much better than the lowest molecular weight H-bonded complex. These results confirm and extend more partial SRG results from previous literature. The PM-IRSAS photoorientation and thermal relaxation data indicate that the azo molecules orient more in i-bonded than in H-bonded complexes. Notably, the maximum orientation parameter achieved during the photoorientation stage ($<P_2>_{max}$), which reached a plateau early on for the H-bonded complexes but continued to rise at the end of the irradiation period for the i-bonded complexes (especially for the lowest degree of polymerization), is about three times greater for the i-bonded complexes than for the H-bonded complexes. The thermal relaxation stage indicates that photoorientation in the i-bonded complexes is more stable than in the H-bonded complexes ($<P_2>_{res}$ about 80-90% vs. 50%).

The kinetics of photoorientation were analyzed by fitting the curves with a biexponential function, from which a fast AHB component and a slow AR component were extracted. These indicate that AHB is the dominant factor at close to 90% in the H-bonded complexes while AR

contributes about 50-70% (decreasing with DP) to photoorientation in the i-bonded complexes. During thermal relaxation, inverse AHB is predominant, while AR is largely inhibited by the high T_g's. By comparison with similar PM-IRSAS data for an analogous H-bonded complex, it was determined that the strong intermolecular azo-azo interactions leading to a liquid crystal structure, rather than the ionic nature of the supramolecular bond or the particularly high T_g of the i-bonded complex, is critical to the photoorientation and relaxation behavior in the i-bonded complex. Furthermore, the presence of significant AR is essential to efficient SRG inscription, at least for the contrarotating circularly polarized (LCP-RCP) patterned irradiation used here. Moreover, the AR process may or may not involve polymer sidegroup orientation. On the other hand, the increasing AR contribution with polymer molecular weight for the i-bonded complexes and its apparent invariance for the H-bonded complexes is not reflected in the SRG curves, which can be rationalized by polymer chain entanglement that hinders long-range polymer motion in the SRG process but to a lesser extent in the shorter length scale motion in AR.

Thus, on a molecular level the inscribed SRG's are the culmination of multiple AR steps, where each step involves the creation of anisotropic free volume to which the neighboring molecules and polymer segments adapt. This process is enhanced by strong azo-azo interactions, as typically present in LC systems, leading to cooperative AR motion. These findings help elucidate the effect of the nature and the strength of the supramolecular interaction as well as the effect of polymer molecular weight on the photoinduced motions (molecular and macroscopic) of azobenzene-containing polymers. These insights are expected to be of benefit to the design of more efficient photoresponsive materials or optical devices.

ASSOCIATED CONTENT

Supporting Information

^{1}H NMR characterization, additional IR spectra, additional SRG inscription results (atomic force microscopy images, diffraction efficiency curves and table of values), additional photoorientation results (spectra, plots, examples of curve fits). The supporting information is available free of charge on the ACS publications website at DOI:…

AUTHOR INFORMATION

Corresponding Authors

* geraldine.bazuin@umontreal.ca

* c.pellerin@umontreal.ca

Author Contributions

The manuscript was written through contributions of all authors. All authors have given approval to the final version of the manuscript.

ACKNOWLEDGEMENTS

This work was supported by the Natural Science and Engineering Research Council of Canada (NSERC, grants RGPIN-2015-04014, RGPIN-2015-05743, and RGPGP/00073-2014) and the Canada Foundation for Innovation. We thank Compute Canada for access to the supercomputer Graham.

REFERENCES

1. Natansohn, A.; Rochon, P., Photoinduced Motions in Azo-Containing Polymers. *Chem. Rev.* **2002,** *102*, 4139-4175.
2. Bandara, H. M.; Burdette, S. C., Photoisomerization in Different Classes of Azobenzene. *Chem. Soc. Rev.* **2012,** *41*, 1809-1825.
3. Mahimwalla, Z.; Yager, K. G.; Mamiya, J.-i.; Shishido, A.; Priimagi, A.; Barrett, C. J., Azobenzene Photomechanics: Prospects and Potential Applications. *Polym. Bull.* **2012,** *69*, 967-1006.

4. Lee, S.; Kang, H. S.; Park, J. K., Directional Photofluidization Lithography: Micro/Nanostructural Evolution by Photofluidic Motions of Azobenzene Materials. *Adv. Mater.* **2012,** *24*, 2069-2103.
5. Viswanathan, N. K.; Kim, D. Y.; Bian, S. P.; Williams, J.; Liu, W.; Li, L.; Samuelson, L.; Kumar, J.; Tripathy, S. K., Surface Relief Structures on Azo Polymer Films. *J. Mater. Chem.* **1999,** *9*, 1941-1955.
6. Karageorgiev, P.; Neher, D.; Schulz, B.; Stiller, B.; Pietsch, U.; Giersig, M.; Brehmer, L., From Anisotropic Photo-Fluidity towards Nanomanipulation in the Pptical Near-Field. *Nature Mater.* **2005,** *4*, 699-703.
7. Miniewicz, A.; Sobolewska, A.; Piotrowski, W.; Karpinski, P.; Bartkiewicz, S.; Schab-Balcerzak, E., Thermocapillary Marangoni Flows in Azopolymers. *Materials* **2020,** *13*, 2264.
8. Sekkat, Z., Model for Athermal Enhancement of Molecular Mobility in Solid Polymers by Light. *Phys. Rev. E* **2020,** *102*, 032501.
9. Rochon, P.; Batalla, E.; Natansohn, A., Optically induced surface gratings on azoaromatic polymer films. *Appl. Phys. Lett.* **1995,** *66*, 136-138.
10. Kim, D. Y.; Tripathy, S. K.; Li, L.; Kumar, J., Laser-induced Holographic Surface Relief Gratings on Nonlinear Optical Polymer Films. *Appl. Phys. Lett.* **1995,** *66*, 1166-1168.
11. Garrot, D.; Lassailly, Y.; Lahlil, K.; Boilot, J. P.; Peretti, J., Real-Time Near-Field Imaging of Photoinduced Matter Motion in Thin Solid Films Containing Azobenzene Derivatives. *Appl. Phys. Lett.* **2009,** *94*, 033303.
12. Yager, K. G.; Barrett, C. J., Photomechanical Surface Patterning in Azo-Polymer Materials. *Macromolecules* **2006,** *39*, 9320-9326.
13. Yadavalli, N. S.; Loebner, S.; Papke, T.; Sava, E.; Hurduc, N.; Santer, S., A Comparative Study of Photoinduced Deformation in Azobenzene Containing Polymer Films. *Soft Matter* **2016,** *12*, 2593-2603.
14. Kumar, J.; Li, L.; Jiang, X. L.; Kim, D.-Y.; Lee, T. S.; Tripathy, S., Gradient force: The mechanism for surface relief grating formation in azobenzene functionalized polymers. *Appl. Phys. Lett.* **1998,** *72*, 2096-2098.
15. Shishido, A., Rewritable Holograms Based on Azobenzene-Containing Liquid-Crystalline Polymers. *Polym. J.* **2010,** *42*, 525-533.
16. Hvilsted, S.; Sánchez, C.; Alcalá, R., The Volume Holographic Optical Storage Potential in Azobenzene Containing Polymers. *J. Mater. Chem.* **2009,** *19*, 6641-6648.
17. Bang, C.-U.; Shishido, A.; Ikeda, T., Azobenzene Liquid-Crystalline Polymer for Optical Switching of Grating Waveguide Couplers with a Flat Surface. *Macromol. Rapid Commun.* **2007,** *28*, 1040-1044.
18. Paterson, J.; Natansohn, A.; Rochon, P.; Callender, C. L.; Robitaille, L., Optically Inscribed Surface Relief Diffraction Gratings on Azobenzene-Containing Polymers for Coupling Light into Slab Waveguides. *Appl. Phys. Lett.* **1996,** *69*, 3318-3320.
19. Stockermans, R. J.; Rochon, P. L., Narrow-Band Resonant Grating Waveguide Filters Constructed with Azobenzene Polymers. *Appl. Opt.* **1999,** *38*, 3714-3719.
20. Fedele, C.; Netti, P. A.; Cavalli, S., Azobenzene-based Polymers: Emerging Applications as Cell Culture Platforms. *Biomater. Sci.* **2018,** *6*, 990-995.
21. Xue, X.; Zhu, J.; Zhang, Z.; Zhou, N.; Tu, Y.; Zhu, X., Soluble Main-Chain Azobenzene Polymers via Thermal 1,3-Dipolar Cycloaddition: Preparation and Photoresponsive Behavior. *Macromolecules* **2010,** *43*, 2704-2712.

22. Fang, L.; Zhang, H.; Li, Z.; Zhang, Y.; Zhang, Y.; Zhang, H., Synthesis of Reactive Azobenzene Main-Chain Liquid Crystalline Polymers via Michael Addition Polymerization and Photomechanical Effects of Their Supramolecular Hydrogen-Bonded Fibers. *Macromolecules* **2013,** *46*, 7650-7660.
23. Lehn, J.-M., *Supramolecular Chemistry: Concepts and Perspectives*. 1st ed.; Wiley-VCH: 1995.
24. Lehn, J.-M., Supramolecular Polymer Chemistry - Scope and Perspectives. *Polym. Int.* **2002,** *51*, 825-839.
25. Binder, W. H.; Zirbs, R., Supramolecular Polymers and Networks with Hydrogen Bonds in the Main- and Side-Chain. *Adv. Polym. Sci.* **2006,** *207*, 1-78.
26. Priimagi, A.; Vapaavuori, J.; Rodriguez, F. J.; Faul, C. F. J.; Heino, M. T.; Ikkala, O.; Kauranen, M.; Kaivola, M., Hydrogen-Bonded Polymer−Azobenzene Complexes: Enhanced Photoinduced Birefringence with High Temporal Stability through Interplay of Intermolecular Interactions. *Chem. Mater.* **2008,** *20*, 6358-6363.
27. Priimagi, A.; Kaivola, M.; Rodriguez, F. J.; Kauranen, M., Enhanced Photoinduced Birefringence in Polymer-Dye Complexes: Hydrogen Bonding Makes a Difference. *Appl. Phys. Lett.* **2007,** *90*, 121103.
28. Priimagi, A.; Lindfors, K.; Kaivola, M.; Rochon, P., Efficient Surface-Relief Gratings in Hydrogen-Bonded Polymer-Azobenzene Complexes. *ACS Appl. Mater. Interfaces* **2009,** *1*, 1183-1189.
29. Koskela, J. E.; Vapaavuori, J.; Ras, R. H. A.; Priimagi, A., Light-Driven Surface Patterning of Supramolecular Polymers with Extremely Low Concentration of Photoactive Molecules. *ACS Macro Lett.* **2014,** *3*, 1196-1200.
30. Gao, J.; He, Y.; Liu, F.; Zhang, X.; Wang, Z.; Wang, X., Azobenzene-Containing Supramolecular Side-Chain Polymer Films for Laser-Induced Surface Relief Gratings. *Chem. Mater.* **2007,** *19*, 3877-3881.
31. Vapaavuori, J.; Valtavirta, V.; Alasaarela, T.; Mamiya, J.-I.; Priimagi, A.; Shishido, A.; Kaivola, M., Efficient Surface Structuring and Photoalignment of Supramolecular Polymer–Azobenzene Complexes through Rational Chromophore Design. *J. Mater. Chem.* **2011,** *21*, 15437-15441.
32. Vapaavuori, J.; Priimagi, A.; Kaivola, M., Photoinduced Surface-Relief Gratings in Films of Supramolecular Polymer–Bisazobenzene Complexes. *J. Mater. Chem.* **2010,** *20*, 5260-5264.
33. Vapaavuori, J.; Goulet-Hanssens, A.; Heikkinen, I. T. S.; Barrett, C. J.; Priimagi, A., Are Two Azo Groups Better than One? Investigating the Photoresponse of Polymer-Bisazobenzene Complexes. *Chem. Mater.* **2014,** *26*, 5089-5096.
34. Zhang, Q.; Bazuin, C. G.; Barrett, C. J., Simple Spacer-Free Dye-Polyelectrolyte Ionic Complex: Side-Chain Liquid Crystal Order with High and Stable Photoinduced Birefringence. *Chem. Mater.* **2008,** *20*, 29-31.
35. Zhang, Q.; Wang, X.; Barrett, C. J.; Bazuin, C. G., Spacer-Free Ionic Dye−Polyelectrolyte Complexes: Influence of Molecular Structure on Liquid Crystal Order and Photoinduced Motion. *Chem. Mater.* **2009,** *21*, 3216-3227.
36. Xiao, S.; Lu, X.; Lu, Q., Photosensitive Polymer from Ionic Self-Assembly of Azobenzene Dye and Poly(ionic liquid) and Its Alignment Characteristic toward Liquid Crystal Molecules. *Macromolecules* **2007,** *40*, 7944-7950.
37. Zhu, X.; Beginn, U.; Moller, M.; Gearba, R. I.; Anokhin, D. V.; Ivanov, D. A., Self-Organization of Polybases Neutralized with Mesogenic Wedge-Shaped Sulfonic Acid

Molecules: An Approach toward Supramolecular Cylinders. *J. Am. Chem. Soc.* **2006,** *128*, 16928-16937.
38. Kulikovska, O.; Goldenberg, L. M.; Stumpe, J., Supramolecular Azobenzene-Based Materials for Optical Generation of Microstructures. *Chem. Mater.* **2007,** *19*, 3343-3348.
39. Shinbo, K.; Baba, A.; Kaneko, F.; Kato, T.; Kato, K.; Advincula, R. C.; Knoll, W., In situ Investigations on the Preparations of Layer-by-Layer Films Containing Azobenzene and Applications for LC Display Devices. *Mater. Sci. Eng., C* **2002,** *22*, 319-325.
40. Priimagi, A.; Cavallo, G.; Metrangolo, P.; Resnati, G., The Halogen Bond in the Design of Functional Supramolecular Materials: Recent Advances. *Acc. Chem. Res.* **2013,** *46*, 2686-2695.
41. Saccone, M.; Dichiarante, V.; Forni, A.; Goulet-Hanssens, A.; Cavallo, G.; Vapaavuori, J.; Terraneo, G.; Barrett, C. J.; Resnati, G.; Metrangolo, P., et al., Supramolecular Hierarchy among Halogen and Hydrogen Bond Donors in Light-Induced Surface Patterning. *J. Mater. Chem. C* **2015,** *3*, 759-768.
42. Stumpel, J. E.; Saccone, M.; Dichiarante, V.; Lehtonen, O.; Virkki, M.; Metrangolo, P.; Priimagi, A., Surface-Relief Gratings in Halogen-Bonded Polymer-Azobenzene Complexes: A Concentration-Dependence Study. *Molecules* **2017,** *22*, 1844.
43. Christopherson, J. C.; Topić, F.; Barrett, C. J.; Friščić, T., Halogen-Bonded Cocrystals as Optical Materials: Next-Generation Control over Light–Matter Interactions. *Cryst. Growth Des.* **2018,** *18*, 1245-1259.
44. Bertani, R.; Metrangolo, P.; Moiana, A.; Perez, E.; Pilati, T.; Resnati, G.; Rico-Lattes, I.; Sassi, A., Supramolecular Route to Fluorinated Coatings: Self-Assembly Between Poly(4-vinylpyridines) and Haloperfluorocarbons. *Adv. Mater.* **2002,** *14*, 1197-1201.
45. Vapaavuori, J.; Bazuin, C. G.; Priimagi, A., Supramolecular Design Principles for Efficient Photoresponsive Polymer–Azobenzene Complexes. *J. Mater. Chem. C* **2018,** *6*, 2168-2188.
46. Vapaavuori, J.; Koskela, J. E.; Wang, X.; Ras, R. H. A.; Priimagi, A.; Bazuin, C. G.; Pellerin, C., Effect of Hydrogen-Bond Strength on Photoresponsive Properties of Polymer-Azobenzene Complexes. *Can. J. Chem.* **2020,** *98*, 531-538.
47. Priimagi, A.; Cavallo, G.; Forni, A.; Gorynsztejn-Leben, M.; Kaivola, M.; Metrangolo, P.; Milani, R.; Shishido, A.; Pilati, T.; Resnati, G., et al., Halogen Bonding versus Hydrogen Bonding in Driving Self-Assembly and Performance of Light-Responsive Supramolecular Polymers. *Adv. Funct. Mater.* **2012,** *22*, 2572-2579.
48. Vapaavuori, J.; Heikkinen, I. T. S.; Dichiarante, V.; Resnati, G.; Metrangolo, P.; Sabat, R. G.; Bazuin, C. G.; Priimagi, A.; Pellerin, C., Photomechanical Energy Transfer to Photopassive Polymers through Hydrogen and Halogen Bonds. *Macromolecules* **2015,** *48*, 7535-7542.
49. Wang, X.; Vapaavuori, J.; Wang, X.; Sabat, R. G.; Pellerin, C.; Bazuin, C. G., Influence of Supramolecular Interaction Type on Photoresponsive Azopolymer Complexes: A Surface Relief Grating Formation Study. *Macromolecules* **2016,** *49*, 4923-4934.
50. Börger, V.; Menzel, H.; Huber, M. R., Influence of the Molecular Weight of Azopolymers on the Photo-Induced Formation of Surface Relief Gratings. *Mol. Cryst. Liq. Cryst* **2005,** *430*, 89-97.
51. Barrett, C. J.; Natansohn, A. L.; Rochon, P. L., Mechanism of Optically Inscribed High-Efficiency Diffraction Gratings in Azo Polymer Films. *J. Phys. Chem.* **1996,** *100*, 8836-8842.
52. Laventure, A.; Bourotte, J.; Vapaavuori, J.; Karperien, L.; Sabat, R. G.; Lebel, O.; Pellerin, C., Photoactive/Passive Molecular Glass Blends: An Efficient Strategy to Optimize

Azomaterials for Surface Relief Grating Inscription. *ACS Appl. Mater. Interfaces* **2017,** *9*, 798-808.
53. Wang, X.; Vapaavuori, J.; Bazuin, C. G.; Pellerin, C., Molecular-Level Study of Photoorientation in Hydrogen-Bonded Azopolymer Complexes. *Macromolecules* **2018,** *51*, 1077-1087.
54. Vapaavuori, J.; Laventure, A.; Bazuin, C. G.; Lebel, O.; Pellerin, C., Submolecular Plasticization Induced by Photons in Azobenzene Materials. *J. Am. Chem. Soc.* **2015,** *137*, 13510-13517.
55. Liang, Y.; Mauran, D.; Prud'homme, R. E.; Pellerin, C., A New Method for the Time-Resolved Analysis of Structure and Orientation: Polarization Modulation Infrared Structural Absorbance Spectroscopy. *Appl. Spectrosc.* **2008,** *62*, 941-947.
56. Moniruzzaman, M.; Talbot, J. D. R.; Sabey, C. J.; Fernando, G. F., The Use of 1H NMR and UV–vis Measurements for Quantitative Determination of Trans/Cis Isomerization of a Photo-responsive Monomer and its Copolymer. *J. Appl. Polym. Sci.* **2006,** *100*, 1103-1112.
57. Karukstis, K. K.; Savin, D. A.; Loftus, C. T.; D'Angelo, N. D., Spectroscopic Studies of the Interaction of Methyl Orange with Cationic Alkyltrimethylammonium Bromide Surfactants. *J. Colloid Interface Sci.* **1998,** *203*, 157-163.
58. Eisenbach, C. D., Effect of Polymer Matrix on the Cis-Trans Isomerization of Azobenzene Residues in Bulk Polymers. *Makromol. Chem.* **1978,** *179*, 2489-2506.
59. Vapaavuori, J.; Ras, R. H. A.; Kaivola, M.; Bazuin, C. G.; Priimagi, A., From Partial to Complete Optical Erasure of Azobenzene–Polymer Gratings: Effect of Molecular Weight. *J. Mater. Chem. C* **2015,** *3*, 11011-11016.
60. Wang, X.; Vapaavuori, J.; Zhao, Y.; Bazuin, C. G., A Supramolecular Approach to Photoresponsive Thermo/Solvoplastic Block Copolymer Elastomers. *Macromolecules* **2014,** *47*, 7099-7108.
61. Lagugné Labarthet, F.; Buffeteau, T.; Sourisseau, C., Analyses of the Diffraction Efficiencies, Birefringence, and Surface Relief Gratings on Azobenzene-Containing Polymer Films. *J. Phys. Chem. B* **1998,** *102*, 2654-2662.
62. Yager, K. G.; Barrett, C. J., Confinement of Surface Patterning in Azo-Polymer Thin Films. *J. Chem. Phys.* **2007,** *126*, 094908.
63. Dumont, M. L.; Sekkat, Z., Dynamical Study of Photoinduced Anisotropy and Orientational Relaxation of Azo Dyes in Polymeric Films: Poling at Room Temperature. *Proc. SPIE* **1993,** *1774*, 188-199.
64. Sekkat, Z.; Dumont, M., Photoassisted Poling of Azo Dye Doped Polymeric Films at Room Temperature. *Appl. Phys. B* **1992,** *54*, 486-489.
65. Sekkat, Z.; Dumont, M., Photoinduced Orientation of Azo Dyes in Polymeric Films. Characterization of Molecular Angular Mobility. *Synth. Met.* **1993,** *54*, 373-381.
66. Blanche, P. A.; Lemaire, P. C.; Dumont, M.; Fischer, M., Photoinduced Orientation of Azo Dye in Various Polymer Matrices. *Opt. Lett.* **1999,** *24*, 1349-1351.
67. Kiselev, A. D.; Chigrinov, V. G.; Kwok, H. S., Kinetics of Photoinduced Ordering in Azo-Dye Films: Two-State and Diffusion Models. *Phys. Rev. E Stat. Nonlin. Soft Matter. Phys.* **2009,** *80*, 011706.
68. Kiselev, A. D.; Chigrinov, V. G.; Pasechnik, S. V.; Dubtsov, A. V., Photoinduced Reordering in Thin Azo-Dye Films and Light-induced Reorientation Dynamics of the Nematic Liquid-Crystal Easy Axis. *Phys. Rev. E Stat. Nonlin. Soft Matter. Phys.* **2012,** *86*, 011706.

69. Sekkat, Z.; Wood, J.; Knoll, W., Reorientation Mechanism of Azobenzenes within the Trans --> Cis Photoisomerization. *J. Phys. Chem.* **1995,** *99*, 17226-17234.
70. Ho, M. S.; Natansohn, A.; Rochon, P., Azo Polymers for Reversible Optical Storage. 7. The Effect of the Size of the Photochromic Groups. *Macromolecules* **1995,** *28*, 6124-6127.
71. Buffeteau, T.; Pézolet, M., In situ Study of Photoinduced Orientation in Azopolymers by Time-dependent Polarization Modulation Infrared Spectroscopy. *Appl. Spectrosc.* **1996,** *50*, 948-955.
72. Diggins, A.; Dawson, E.; Kamaliardakani, M.; Pellerin, C.; Sabat, R. G.; Lebel, O., Azobenzene Molecular Glasses with Tuned Glass Transition Temperatures: From Optimal Light-induced Motion to Self-erasable Gratings. *J. Mater. Chem. C* **2020,** *8*, 6203-6213.
73. Singleton, T. A.; Ramsay, K. S.; Barsan, M. M.; Butler, I. S.; Barrett, C. J., Azobenzene Photoisomerization under High External Pressures: Testing the Strength of a Light-Activated Molecular Muscle. *J. Phys. Chem. B* **2012,** *116*, 9860-9865.
74. Ishitobi, H.; Akiyama, T.; Sekkat, Z.; Inouye, Y., Optical Trapping of Photosoftened Solid Polymers. *J. Phys. Chem. C* **2020,** *124*, 26037-26042.

Molecular-Level Photoorientation Insights into Macroscopic Photoinduced Motion in Azobenzene-Containing Polymer Complexes

Mahnaz Kamaliardakani,[1] Jaana Vapaavuori,[1,†] Xiaoxiao Wang,[1] Ribal Georges Sabat,[2] C. Geraldine Bazuin,[*,1] Christian Pellerin[*,1]

TOC graphic